ACCOUNTS
of chemical research

Endohedral Metal Atoms in Pristine and Functionalized Fullerene Cages

MICHIO YAMADA, TAKESHI AKASAKA,* AND SHIGERU NAGASE*

Center for Tsukuba Advanced Research Alliance, University of Tsukuba, Tsukuba, Ibaraki 305-8577, Japan, and Department of Theoretical and Computational Molecular Science, Institute for Molecular Science, Okazaki, Aichi 444-8585, Japan

RECEIVED ON MAY 3, 2009

CONSPECTUS

Fullerene, an allotropic form of carbon made up of spherical molecules formed from pentagonal and hexagonal rings, was first discovered in 1985. Because fullerenes have spacious inner cavities, atoms and clusters can be encapsulated inside the fullerene cages to form endohedral fullerenes.

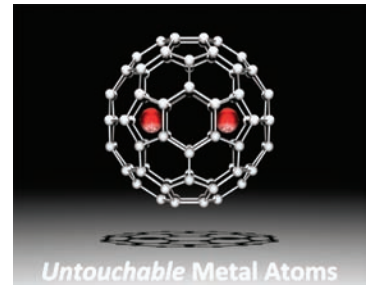

In particular, the unique structural and electronic properties of endohedral metallofullerenes (EMFs), where metal atoms are encapsulated within the fullerene, have attracted wide interest from physicists and chemists as well as materials scientists and biologists. The remarkable characteristics of these molecules originate in the electron transfer from the encapsulated metal atoms to the carbon cage. The positions and movements of the encapsulated metal atoms are important determinants of the chemical and physical properties of EMFs.

In this Account, we specifically describe the positions and dynamic behavior of the metal atoms encapsulated in pristine and functionalized fullerene cages. First, we examined whether the metal atoms are attached rigidly to cage carbons or move around. Our systematic investigations of EMFs, including $M@C_{2v}$–C_{82}, $M_2@D_2(10611)$–C_{72}, $M_2@D_{3h}(5)$–C_{78}, $M_2@I_h$–C_{80}, and $M_2@D_{5h}$–C_{80}, revealed that the metal positions and movements vary widely with different cage structures and numbers of metal atoms.

Second, we wanted to understand whether we could control the positions and movements of the *untouchable* metal atoms in EMFs. One possible way to modulate this behavior was through attachment of a molecule to the outer surface of the cage. We developed synthetic methods to modify EMFs and have examined the metal positions and movements in the functionalized carbon cages. Remarkably, we could alter the dynamic behavior of the encaged metal atoms in $M_2@I_h$–C_{80} drastically through chemical modification of the outer cage. We anticipate that the control of metal atom structures and dynamics within a cage could be valuable for designing functional molecular devices with new electronic or magnetic properties.

1. Introduction

Fullerene, an allotropic form of carbon, was first discovered serendipitously in 1985 during the course of mass spectroscopic studies of pulsed laser vaporization of graphite.[1] Fullerenes are spherical molecules made of pentagonal and hexagonal carbon rings. Because fullerenes have spacious inner cavities, atoms and clusters can be encapsulated inside the fullerene cages to form endohedral fullerenes. In particular, encapsulation of metal atoms offers a new class of hybrid molecules, so-called endohedral metallofullerenes (EMFs).[2] Since the first discovery of lanthanum-containing EMFs in 1991,[3] their use has been extended into areas of chemistry and physics, in addition to advanced materials[4−7] and medicinal sciences[8,9] because of their unique properties. The presence of the electron transfer from the metal atoms to the carbon cage imparts remarkable characteristics to EMFs. Recently, cage frameworks have been verified using ^{13}C nuclear magnetic resonance (NMR) spectroscopic studies. Even so,

Published on the Web 09/03/2009 www.pubs.acs.org/acr
10.1021/ar900140n

many potentially important and intriguing problems remain. In this regard, the determination of the metal positions is a matter of great importance because the metal positions strongly affect the chemical and physical properties of EMFs. It has been generally accepted that extractable EMFs take on endohedral structures. However, definitive proof of the structure must be performed for each EMF. In particular, it is worth clarifying whether metal atoms are attached rigidly to fullerene cages or move around because the control of the positions and movements of the metal atoms in EMFs would help in designing functional devices for molecular electronics. Moreover, organic functionalization of EMFs will be an important direction for the synthesis of further novel materials.

This Account summarizes ongoing efforts to synthesize and characterize various kinds of EMFs and functionalized EMFs systematically and to explore dynamic behaviors of the metal atoms inside carbon cages using single-crystal X-ray crystallography, NMR spectroscopy, and theoretical calculations. We have specifically examined lanthanum-, cerium-, and gadolinium-containing EMFs because they can be considered as prototypes among EMFs of many kinds. Throughout this Account, guidelines for evaluating and controlling the positions and movements of *untouchable* metal atoms inside fullerene cages will be provided.

2. Preparation of EMFs

EMFs are synthesized in a modified Krätschmer−Huffman generator during the vaporization of graphite rods containing metal oxides in a helium atmosphere by arc-discharge. By this way, complex mixtures of empty fullerenes and EMFs mixed together in a carbonaceous soot matrix are obtained. The percentage of fullerenes and EMFs in the raw soot is normally less than 10%. Among them, EMFs can be obtained by the extraction with organic solvents, followed by multi-step high-performance liquid chromatography (HPLC) procedures. The total yield of purified EMFs is generally lower than 1%.

3. Monometallofullerene M@C_{2v}−C_{82}

Actually, M@C_{2v}−C_{82} (M = Group 3 metals and lanthanides) have been known as representative monometallofullerenes. The electron transfer of three valence electrons creates an open-shell electronic structure, formally described as $M^{3+}(C_{2v}-C_{82})^{3-}$. Their paramagnetic nature has obstructed NMR spectroscopic studies of them. In this context, electrochemical reduction of the paramagnetic EMFs[10−14] has enabled measurement of the ^{13}C NMR spectra of their anions to determine the cage framework. To verify the metal position in M@C_{2v}−C_{82}, we specifically examined the paramagnetic effects caused by a f electron on the Ce ($4f^15d^16s^2$) atom in Ce@C_{2v}−C_{82}, which provides information related to the metal position, by analyzing ^{13}C NMR shifts of its anion.

First, we described the mapping of the bond connectivity in $[Ce@C_{2v}-C_{82}]^-$ and fully assigned the NMR lines by 2D INADEQUATE NMR measurements.[15] This complete assignment enables us to analyze the following paramagnetic NMR shifts, which are induced by the f electron on the Ce atom. All carbon chemical shifts (δ) show considerable temperature dependence originating from the f-electron spin. The chemical shifts of paramagnetic molecules in solution are generally expressed as a sum of three contributions from diamagnetic (δ_{dia}), Fermi contact (δ_{fc}), and pseudo-contact (δ_{pc}) shifts, where the paramagnetic δ_{fc} and δ_{pc} are proportional to T^{-1} and T^{-2} (T = absolute temperature), respectively.[16] The δ_{dia} values correspond to the chemical shifts of the diamagnetic $[La@C_{2v}-C_{82}]^-$.[17] The δ_{pc} makes a much larger contribution than δ_{fc}, as is apparent from the fact that no significant connection exists between the Ce atom and cage carbons. Therefore, the chemical shifts of cerium metallofullerenes are expressed briefly as eq 1, where r is the distance between Ce and cage carbons, θ is the angle between the **r** vector and the C_2 axis of Ce@C_{2v}−C_{82}, and C is a common constant with a negative value for all cage carbons.

$$\delta = \delta_{dia} + \frac{C(3\cos^2\theta - 1)}{r^3T^2} \quad (1)$$

It is noteworthy that δ_{pc} includes geometrical information (r and θ) related to the encapsulated Ce atoms. To obtain the optimal distance (x) between Ce and the center of the hexagonal ring along the C_2 axis, full geometry optimization was conducted for $[Ce@C_{2v}-C_{82}]^-$ using density functional theory (DFT). The optimal x is 2.063 Å when the Ce atom is located near the hexagonal ring (Figure 1). In addition, the optimal x values are scarcely changed for neutral Ce@C_{2v}−C_{82}. The x value was obtained experimentally as 2.1−2.8 Å using paramagnetic NMR shift analysis. Therefore, we conclude that the Ce atom in Ce@C_{2v}−C_{82} as well as $[Ce@C_{2v}-C_{82}]^-$ is located at an off-center position adjacent to a hexagonal ring along the C_2 axis of the cage. This metal position corresponds to the minima of the electrostatic potential of C_{2v}−C_{82}.[3−18] This agreement underscores that the electrostatic metal−cage interaction plays a dominant role in both stabilizing the endohedral structure and determining the metal position.

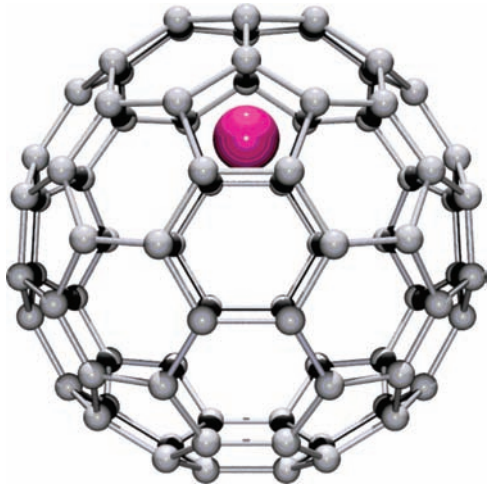

FIGURE 1. Optimized structure of $[Ce@C_{2v}-C_{82}]^-$.

4. Functionalized Derivatives of M@C_{2v}−C_{82}

Because 24 non-equivalent carbons in M@C_{2v}−C_{82} exist, an addition reaction might take place at several sites to yield several possible monoadduct isomers.[19,20] In contrast, the addition reaction of La@C_{2v}−C_{82} with adamantylidene (Ad) carbene affords only one dominant isomer of La@C_{2v}−C_{82}(Ad) (Scheme 1 and Figure 2a).[21] The C−C bond on the addition site was cleaved by adding the electrophilic carbene to form the [6,6] open structure. The Mulliken charge densities and π orbital axis vector (POAV) values are found to be large for the carbons in the hexagonal ring nearest the La atom. We consider that the carbene selectively attacks one of the six electron-rich strained carbons to form the [6,6] open adduct. The La atom is changed slightly by the carbene addition and is located at a single site nearest the addition site.

Similarly, Gd@C_{2v}−C_{82}(Ad) was synthesized (Scheme 1 and Figure 2b).[22] It is notable that the Gd atom is located at an off-center position near a hexagonal ring in the cage, as found for La@C_{2v}−C_{82}(Ad). The Gd position in Gd@C_{2v}−C_{82}(Ad) is closer to the carbon cage than that of the La atom in La@C_{2v}−C_{82}(Ad). Because the carbene addition to La@C_{2v}−C_{82} engenders a slight change of the La position, it is reasonable to consider that the Gd atom in Gd@C_{2v}−C_{82} is also located at an off-center position near a hexagonal ring along the C_2 axis, as are La@C_{2v}−C_{82} and Ce@C_{2v}−C_{82}. This consideration is supported by recent computational[23−25] and X-ray absorption near-edge structure (XANES)[26] studies, although these results are not consistent with the MEM/Rietveld analysis.[27]

The Bingel−Hirsch reaction is a widely applied reaction in fullerene chemistry. We applied the reaction to La@C_{2v}−C_{82} with bromomalonate, in which a singly bonded monoadduct La@C_{2v}−C_{82}CBr($COOC_2H_5$)$_2$ was yielded as the major product (Scheme 1 and Figure 2c).[28,29] The bromomalonate group is singly bonded to the carbon atom on the cage, which is far from the La atom. We assume that the carbanion attacked the most positively charged and second strained carbon atom on the cage, with subsequent oxidation to afford the diamagnetic product. The metal position in La@C_{2v}−C_{82}CBr($COOC_2H_5$)$_2$ is almost identical to that in La@C_{2v}−C_{82}. This finding is acceptable because the addition site is distant from the metal atom, which causes little change of circumstances near the metal atom. When malonate was subjected to the reaction instead of bromomalonate, bis-addition proceeded in a highly regioselective way and engendered the dominant formation of a single bis-adduct isomer, La@C_{2v}−C_{82}[CH($COOC_2H_5$)$_2$]$_2$ (Scheme 1 and Figure 2d).[30] The bis-adduct retains an open-shell electronic structure and crystallizes to form a dimer. The La positions are off the C_2 axis and move slightly toward the hemisphere that undergoes bis-addition.

The photoirradiation of La@C_{2v}−C_{82} with α,α,2,4-tetrachlorotoluene afforded two regioisomers of the radical coupling products, La@C_{2v}−C_{82}CHCl$C_6H_3Cl_2$ (Scheme 1).[31] The X-ray crystallographic analysis was performed for one isomer to disclose its structure (Figure 2e). The La position in the isomer is off the C_2 axis and moves slightly against the hemisphere that undergoes a coupling reaction. This trend contrasts with the case of La@C_{2v}−C_{82}CBr($COOC_2H_5$)$_2$.

5. Dimetallofullerenes $M_2@C_n$ (n = 72, 78, and 80)

With regard to dimetallofullerenes, not only the electrostatic metal−cage interaction but also the electrostatic metal−metal interaction is crucial for the positions and movements of the metal atoms. We synthesized a series of cerium-containing dimetallofullerenes and performed paramagnetic NMR shift analyses to elucidate the behavior of the metal atoms.

The smallest cerium-containing dimetallofullerene, $Ce_2@D_2(10611)-C_{72}$, was first isolated in 2001 by Dunsch and co-workers.[32] In 2008, we elucidated the cage frameworks and the metal positions using NMR spectroscopy (Figure 3a).[33] It is particularly interesting that $Ce_2@D_2(10611)-C_{72}$ does not obey the isolated-pentagon rule (IPR). It is expected that the Ce atoms stabilize the non-IPR cage containing two fused pentagons. In fact, the paramagnetic NMR shift analysis clarified that the Ce atoms face the two fused pentagons on the two poles of the $D_2(10611)-C_{72}$ cage. Indeed, the ^{13}C NMR signals of the fused pentagons are strongly shifted with a decreasing temperature because of the paramagnetic effects of the facing Ce atoms.

SCHEME 1

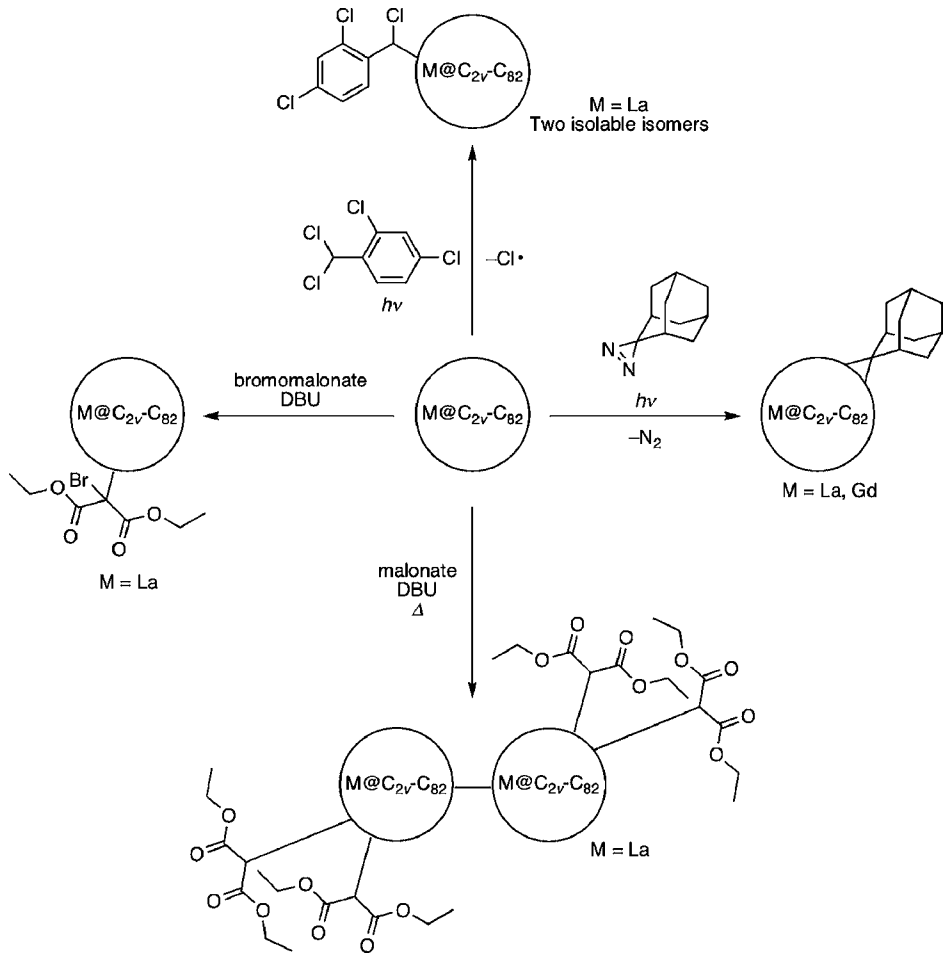

A $D_{3h}(5)$–C_{78} cage also encapsulates two Ce atoms inside to form $Ce_2@D_{3h}(5)$–C_{78}.[34] All carbon chemical shifts show considerable temperature dependence originating from the f-electron spins remaining on the Ce atoms. The paramagnetic NMR shift analysis disclosed that the Ce atoms in $Ce_2@D_{3h}(5)$–C_{78} are localized on the C_3 axis of the ellipsoidal cage. This result agrees well with the optimized structure of $La_2@D_{3h}(5)$–C_{78} calculated using the DFT method (Figure 3b).

Particularly remarkable is the case of $M_2@I_h$–C_{80}, in which the metal atoms circulate three-dimensionally. The circuit of two La^{3+} cations produces a magnetic field at the positions of La. In the ^{139}La NMR study, this should be reflected in the nuclear magnetic relaxation rate and, therefore, the line width. Ordinarily, the interaction between nuclear spins and the induced magnetic field (a spin–rotation interaction) does not contribute significantly to the relaxation time in solution because the molecular rotation is dominantly quenched by neighbors. For $La_2@I_h$–C_{80}, however, the rotation of the La atoms can be preserved because of the unique cage protection, so that the spin–rotation interaction has a drastic effect on the relaxation process. The relaxation caused by the spin–rotation interaction engenders an increase in line width with increasing temperature. This is quite unlike relaxation of other types. Actually, we observed large broadening of the ^{139}La NMR line width with an increasing temperature from 305 to 363 K.[35] That constituted the first experimental evidence for the circular motion of metal atoms in a fullerene cage. In addition, the ^{13}C NMR spectrum of $La_2@I_h$–C_{80} showed only two carbon signals with an intensity ratio of 3:1, indicating delocalization of the two La atoms.[36] The circulation is also supported by theoretical studies. The electrostatic potential map of I_h–C_{80}^{6-} shows almost concentric circles with no clear minima, reflecting the round cage structure.[37] The rotational barrier of the La atoms is calculated as 4.9 kcal/mol. However, the detailed trajectory remains controversial.[38,39]

Similar circulation of metal atoms is also apparent in $Ce_2@I_h$–C_{80} (Figure 3c). The presence of only two signals with a 3:1 intensity ratio in the ^{13}C NMR spectrum of $Ce_2@I_h$–C_{80} indicates that the Ce atoms circulate randomly, as La does in

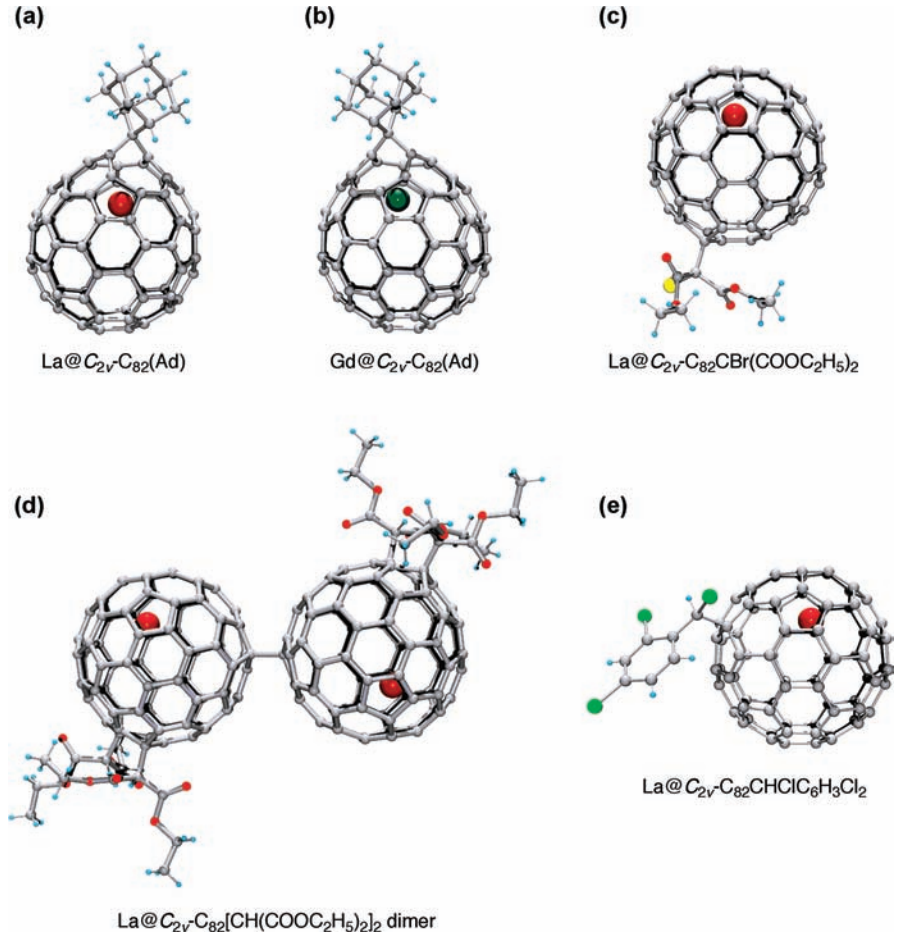

FIGURE 2. X-ray structures of functionalized derivatives of M@C_{2v}−C_{82}.

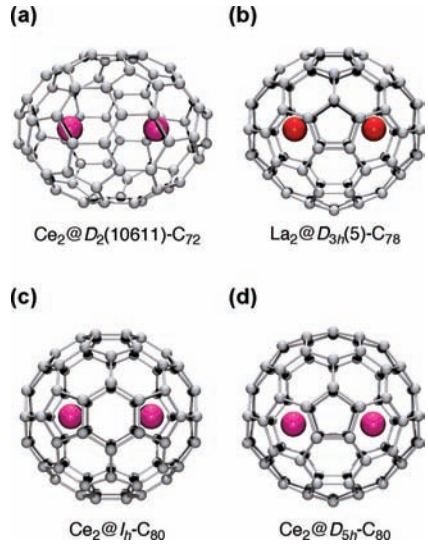

FIGURE 3. Optimized structures of (a) Ce$_2$@D_2(10611)−C_{72}, (b) La$_2$@D_{3h}(5)−C_{78}, (c) Ce$_2$@I_h−C_{80}, and (d) Ce$_2$@D_{5h}−C_{80}.

La$_2$@I_h−C_{80}.[40] The ^{13}C NMR signals show very slight temperature dependence compared to those of Ce$_2$@D_2(10611)−C_{72} and Ce$_2$@D_{3h}(5)−C_{78}, despite the fact that two Ce atoms having f electrons are inside as well. This observation results from the three-dimensional circulation of the Ce atoms, which causes delocalization of the f electrons, thereby reducing the paramagnetic effects.

Very recently, we synthesized Ce$_2$@D_{5h}−C_{80}, which is an isomer of Ce$_2$@I_h−C_{80} (Figure 3d).[41] Paramagnetic NMR shift analysis, together with theoretical calculations, revealed that the Ce atoms circulate two-dimensionally along a band of 10 contiguous hexagons inside a D_{5h}−C_{80} cage, which contrasts sharply to the three-dimensional circulation of the Ce atoms inside an I_h−C_{80} cage.

6. Functionalized Derivatives of La$_2$@D_2(10611)−C_{72} and M$_2$@D_{3h}(5)−C_{78}

A non-IPR fullerene La$_2$@D_2(10611)−C_{72} was modified using a photolytic reaction with diazirine (Scheme 2).[42] The addition of adamantylidene carbene to La$_2$@D_2(10611)−C_{72} occurred at the fused pentagons. Six isomers of La$_2$@D_2(10611)−C_{72}(Ad) were isolated and characterized, among which the structures of the three most abundant isomers (designated as isomer B, isomer C, and isomer D) were elucidated using X-ray crystallography (panels a−c of Figure 4). The

SCHEME 2

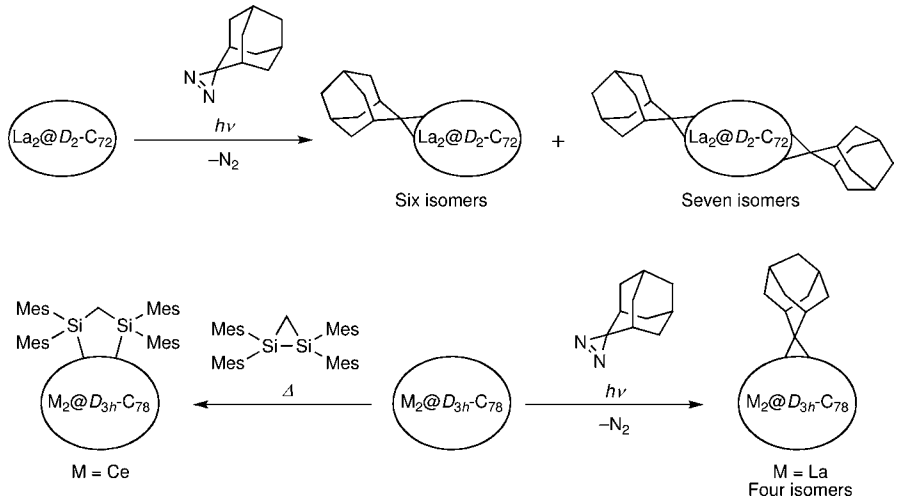

hemisphere on which Ad is not attached seems to remain unchanged in the three isomers, indicating that the addition to a bond far from the [5,5]-bond junction has little effect on the strong interaction between the metal atom and the fused pentagon bond. It is particularly interesting that the La atoms close to the Ad moieties in these isomers move from positions on the [5,5] bonds to the cavities of the broken pentagons. These results suggest that the breaking of a bond close to the [5,5] junction affects the position of the adjacent metal atoms.

By modifying the reaction condition, seven isomers of bis-carbene adducts, $La_2@D_2(10611)-C_{72}(Ad)_2$, were synthesized (Scheme 2). Among these, the structure of the most abundant isomer was clarified using X-ray crystallography (Figure 4d).[43] The La atoms are situated close to the cavities of the broken pentagons. The La−La distance of 4.300 Å is longer than those for the monoadducts (4.171−4.178 Å), which indicates that the two open parts help to relieve the strong repulsion between the two La cations.

Bis-silylation reaction of $Ce_2@D_{3h}(5)-C_{78}$ proceeded smoothly to form a single isomer of $Ce_2@D_{3h}(5)-C_{78}(Mes_2Si)_2CH_2$ (Scheme 2 and Figure 4e).[34] The bis-silylated adduct results from the 1,4-addition of the disilirane to the cage. The Ce atoms are located at two positions directed toward the hexagonal ring at the C_3 axis of the ellipsoidal cage, reflecting that these positions are energetically the most stable. The consider-

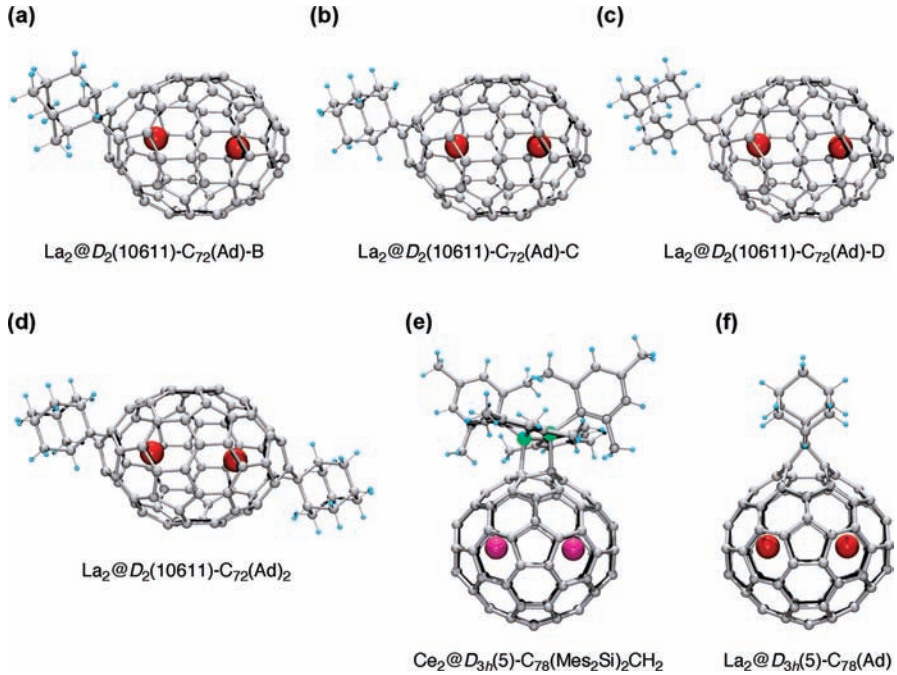

FIGURE 4. X-ray structures of functionalized derivatives of $La_2@D_2(10611)-C_{72}$ and $M_2@D_{3h}(5)-C_{78}$.

SCHEME 3

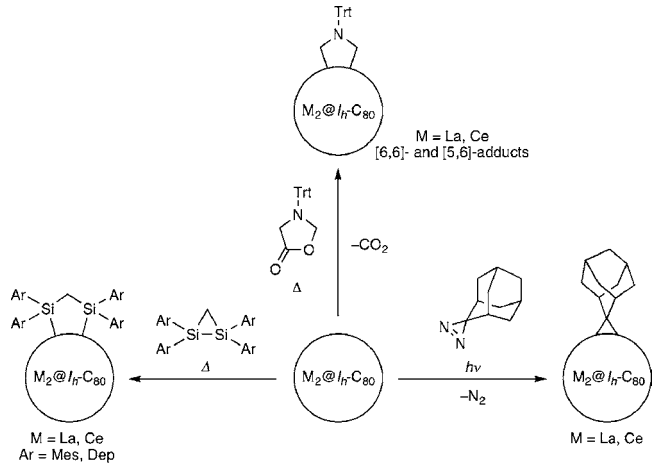

ably long Ce−Ce distance of 4.036 Å in $Ce_2@D_{3h}(5)$−$C_{78}(Mes_2Si)_2CH_2$ results from the electrostatic repulsion between the Ce atoms at the C_3 axis, where the repulsion is minimized. For the bis-silylated adduct, the observed carbon signals show large temperature dependence, as compared to the pristine $Ce_2@D_{3h}(5)$−C_{78} case, which indicates that the two Ce atoms are more tightly localized in the bis-silylated adduct than in pristine $Ce_2@D_{3h}(5)$−C_{78}.

The addition reaction of $La_2@D_{3h}(5)$−C_{78} with adamantylidene carbene afforded four isomers of the monoadduct $La_2@D_{3h}(5)$−C_{78}(Ad) (Scheme 2).[44] The X-ray study shows that one monoadduct has a [5,6] open structure with two La atoms on the C_3 axis of the cage with the La−La distance of 4.081 Å (Figure 4f). The metal positions are almost identical to those in pristine $La_2@D_{3h}(5)$−C_{78},[45] although the C−C bond on the cage is cleaved by the reaction. In this respect, the C−C bond cleavage far from the metal atoms has little effect on the metal position.

7. Positional Control of the Metal Atoms in $M_2@I_h$−C_{80} by Exohedral Chemical Functionalization

More drastic changes of the movements of the metal atoms are observed in functionalized derivatives of $M_2@I_h$−C_{80}. The bis-silylation of $Ce_2@I_h$−C_{80} with disilirane took place quantitatively to afford a single isomer of $Ce_2@I_h$−$C_{80}(Mes_2Si)_2CH_2$, which results from the 1,4-addition of the disilirane (Scheme 3).[40] It is particularly interesting that the X-ray crystallographic analysis of $Ce_2@I_h$−$C_{80}(Mes_2Si)_2CH_2$ showed that the two Ce atoms are localized at two positions directing the hexagonal ring at the equator (Figure 5a). Additionally, six ^{13}C signals are highly shifted by decreasing temperatures from 303 to 253 K in the ^{13}C NMR measurements. This result is explainable by the fact that each Ce atom is directed toward a hexagonal ring at the equator of the cage, as revealed in the X-ray crystal structure. The ^{13}C signals of the sp^3 carbon atoms on the cage are not shifted considerably by the paramagnetic effects. This report constitutes the first experimental evidence for control of the motion of encapsulated atoms inside a fullerene cage. The Ce−Ce distance of 3.829 Å in $Ce_2@I_h$−$C_{80}(Mes_2Si)_2CH_2$ is shorter than that in $Ce_2@D_{3h}(5)$−$C_{78}(Mes_2Si)_2CH_2$. However, the average distance of 2.521 Å between the Ce atoms and the nearest carbon atoms in $Ce_2@I_h$−$C_{80}(Mes_2Si)_2CH_2$ differs little from that of 2.510 Å in $Ce_2@D_{3h}(5)$−$C_{78}(Mes_2Si)_2CH_2$. Subsequently, we synthesized bis-silylated derivatives of $La_2@I_h$−C_{80}, $La_2@I_h$−$C_{80}(Ar_2Si)_2CH_2$ (Ar = Mes and Dep, Dep = 2,6-diethylphenyl) (Scheme 3).[36] The metal positions in $La_2@I_h$−$C_{80}(Dep_2Si)_2CH_2$ closely resemble those in $Ce_2@I_h$−$C_{80}(Mes_2Si)_2CH_2$ with the La−La distance of 3.792 Å, despite the fact that substituents and metals mutually differ (Figure 5b). The ^{139}La NMR measurements taken at various temperatures revealed the dynamic behavior of the encaged La atoms inside the bis-silylated cage. We observed large broadening of the ^{139}La NMR line width with increasing temperature from 183 to 308 K, as derived from the spin−rotation relaxation. This observation indicates that the two La atoms do not stand still but instead hop inside the bis-silylated cage in solution. Because two Ce atoms in $Ce_2@I_h$−$C_{80}(Mes_2Si)_2CH_2$ have restricted movement, we conclude that the two La atoms in $La_2@I_h$−$C_{80}(Ar_2Si)_2CH_2$ hop two-dimensionally along the equator of the bis-silylated cage. This hopping motion is supported by results of theoretical studies that preceded the experimental observations.[46] The strong electron-donating character of the silyl group gives ca. 0.9 electron to the cage, where the electrostatic potential is transformed.

The 1,3-dipolar cycloaddition of $M_2@I_h$−C_{80} afforded [6,6] and [5,6] adducts of endohedral pyrrolidinodimetallofullerene $M_2@I_h$−$C_{80}(CH_2)_2NTrt$ (M = La and Ce) (Scheme 3).[47,48] In particular, the structures of the [6,6]-$La_2@I_h$−$C_{80}(CH_2)_2NTrt$ and [6,6]-$Ce_2@I_h$−$C_{80}(CH_2)_2NTrt$ were elucidated unambiguously using X-ray crystallography (panels c and d of Figure 5). The metal positions in the pyrrolidinodimetallofullerenes were determined using paramagnetic NMR shift analyses. The two metal atoms are fixed at slantwise positions on the mirror plane in the [6,6]-pyrrolidinodimetallofullerenes, whereas the metal atoms are collinear with the pyrrolidine ring in the [5,6]-pyrrolidinodimetallofullerenes. The metal positions in [6,6] and [5,6] adducts are explainable by the electrostatic potential maps inside the corresponding pyrrolidino cages. This finding indicates that the metal positions can be controlled by the

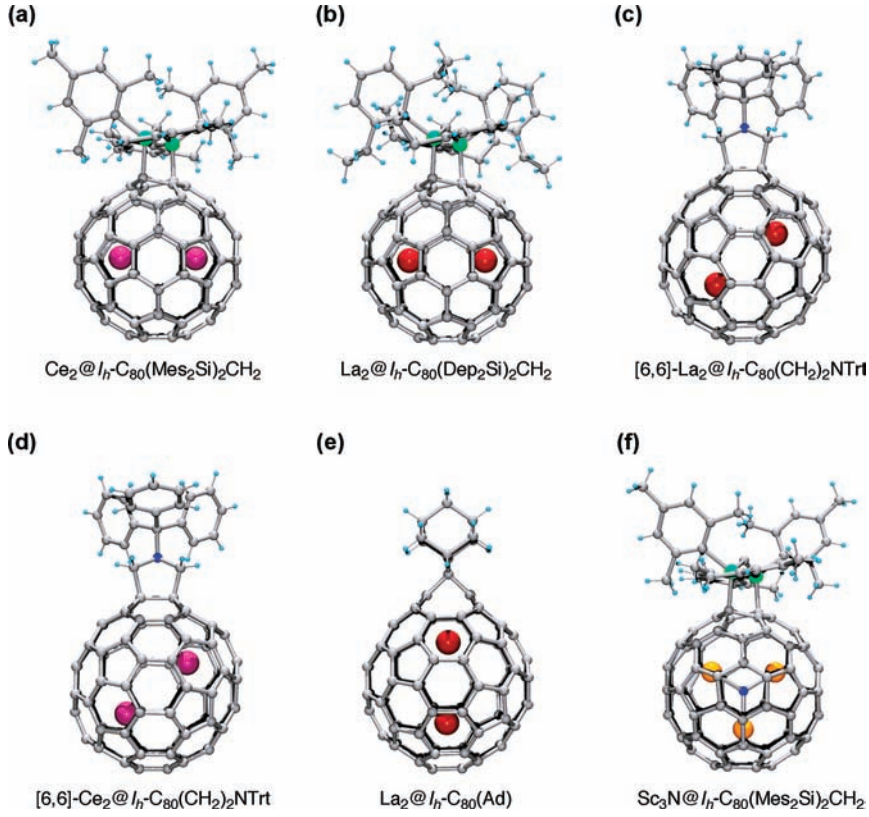

FIGURE 5. X-ray structures of functionalized $M_2@I_h-C_{80}$ and $Sc_3N@I_h-C_{80}$.

addition positions of the addends. The metal distance in [6,6]-$La_2@I_h-C_{80}(CH_2)_2$NTrt (La−La = 3.823 Å) is shorter than that in [6,6]-$Ce_2@I_h-C_{80}(CH_2)_2$NTrt (Ce−Ce = 3.900 Å).

Selective addition of the adamantylidene carbene to $M_2@I_h-C_{80}$ occurs at the [6,6] bond junction with the bond cleavage to afford the formation of the [6,6] open adduct, $M_2@I_h-C_{80}$(Ad) (Scheme 3).[49] Crystallographic data for $La_2@I_h-C_{80}$(Ad) reveals that the two La atoms are collinear with the spiro carbon of the adduct, unlike the three-dimensional random motion in $La_2@I_h-C_{80}$ (Figure 5e). Furthermore, the La−La distance is highly elongated to 4.031 Å, whereas the calculated La−La distance in $La_2@I_h-C_{80}$ is 3.828 Å.[39] The remarkable La−La elongation in $La_2@I_h-C_{80}$(Ad) results from the expansion of the inner space of the cage caused by the bond cleavage, which reduces the electrostatic repulsion between the positively charged La atoms. The elongation engenders the regulation of metal atoms from three-dimensional movement to the restricted behavior. The unique La positions were confirmed using DFT calculations. Paramagnetic ^{13}C NMR spectral analysis of $Ce_2@I_h-C_{80}$(Ad) indicates that the Ce positions are also regulated at room temperature in solution, as found for $La_2@I_h-C_{80}$(Ad).

We expect that controlling the movement of the atom in the cage would be applicable for molecular electronic or magnetic devices, because the restricted movement of the positively charged metal atoms enhances anisotropic properties in terms of the molecular electronic conductance and magnetic moments. It is also noteworthy that these compounds are potential photovoltaic materials, where the orientation of metal atoms may contribute to the efficiencies of the carrier transport.

In a related work, we synthesized a bis-silylated clusterfullerene, $Sc_3N@I_h-C_{80}(Mes_2Si)_2CH_2$.[50,51] The circular motion of the Sc_3N cluster is restricted by the exohedral addition. The X-ray structure shows that the cluster is perpendicular to the equatorial plane of the bis-silylated cage (Figure 5f), which is in sharp contrast to the metal positions in bis-silylated $M_2@I_h-C_{80}$. Restricted movements of encapsulated clusters were also found for the carbene derivatives of $Sc_3C_2@I_h-C_{80}$[52] and $Sc_2C_2@C_{3v}-C_{82}$.[53] Dorn and co-workers reported X-ray structures of [6,6] and [5,6] regioisomers of $Sc_3N@I_h-C_{80}(CH_2)_2$NTrt.[54] It is particularly interesting that the presence of 15 sites for scandium atoms is observed in [6,6]-$Sc_3N@I_h-C_{80}(CH_2)_2$NTrt. On the other hand, only two sets of the cluster are observed in [5,6]-$Sc_3N@I_h-C_{80}(CH_2)_2$NTrt. The cluster movement is not always consistent with that of metal atoms in the corresponding functionalized dimetallofullerenes. That inconsistency results from the difference in the electronic structures and charge distributions of whole molecules between clusterfullerenes and dimetallofullerenes.[50] In addi-

tion, the electrostatic interactions inside the cages differ. With regard to dimetallofullerenes, two metal cations are not bonded and are repulsive of each other. In contrast, clusters have a complicated charge distribution. For that reason, it is difficult to explain the positions of the clusters in clusterfullerenes using the electrostatic potential maps inside the anionic cage.

8. Conclusions

Cationic metal atoms are localized at specific positions where these atoms are stabilized. The metal positions can be predicted by calculating the electrostatic potential maps inside the anionic cages because the metal−cage interaction is considerably ionic. Paramagnetic NMR shift analysis is a powerful method to identify the metal positions in EMFs experimentally. Theoretical predictions are consistent with the experimental results, even when the metal atom has additional f electrons. With regard to dimetallofullerenes, electrostatic repulsion between the metal atoms must be considered. The metal atoms in dimetallofullerenes are located with the longest metal−metal distance, where the electrostatic repulsion is minimized. A peculiar example is $M_2@I_h$−C_{80}, which has the highest symmetry, where the metal atoms rotate three-dimensionally. The electrostatic potential map of I_h−C_{80}^{6-} shows almost concentric circles with no clear minimum. Accordingly, the nonstabilized metal atoms can execute dynamic movement.

Chemical functionalization of EMFs can regulate metal positions and movements of the metal atoms. The metal positions are affected by the addition of addends because the electronic structure of the cage is altered. The positional change is conspicuous when the C−C bond on the cage is cleaved by the reaction. In this case, the metal atoms tend to move to the cleaved site, although in general, the positional change is not extensive. A unique exception is the case of $M_2@I_h$−C_{80}. Chemical functionalization of $M_2@I_h$−C_{80} leads metal atoms with three-dimensional movement into localization at specific positions. The metal positions in the functionalized $M_2@I_h$−C_{80} depend upon the addends, addition positions, and addition forms. Calculation of the electrostatic potential map is useful to predict the metal positions in the functionalized cages. In addition, the electrostatic repulsion between the metal atoms plays an important role in the metal positions. Distances between the metal atoms in functionalized fullerene cages depend upon not only the cage sizes and symmetries but also the addends. The metal distance between the metal atoms in the functionalized I_h−C_{80} cages is shorter than those in the functionalized $D_{3h}(5)$−C_{78} and $D_2(10611)$−C_{72} cages. Carbene addition strongly leads to elongation of the metal distance. The 1,3-dipolar cycloaddition also causes some elongation effect. On the other hand, bis-silylation gives little change of the metal distance. We believe that these systematic studies of the metal atoms in pristine and functionalized EMFs will contribute to a comprehensive understanding of EMFs and future fruitful applications.

This work was supported in part by a Grant-in-Aid for Scientific Research on Innovative Areas (20108001, "pi-Space"), a Grant-in-Aid for Scientific Research (A) (20245006), The Next Generation Super Computing Project (Nanoscience Project), Nanotechnology Support Project, and a Grant-in Aid for Scientific Research on Priority Areas (20036008 and 20038007) from the Ministry of Education, Culture, Sports, Science, and Technology of Japan. M.Y. Thanks the Japan Society for the Promotion of Science (JSPS) for the Research Fellowship for Young Chemists.

BIOGRAPHICAL INFORMATION

Michio Yamada, born in 1981 in Osaka, grew up in Tokyo, Japan. He received his Ph.D. degree from the University of Tsukuba in 2008 under his advisor, Prof. Takeshi Akasaka. He is currently a postdoctoral fellow in the group of Prof. François Diederich at ETH Zürich, Switzerland. His research interests are related to the chemistry of carbon-rich architectures, such as those of fullerenes, metallofullerenes, and acetylenic scaffolds.

Takeshi Akasaka was born in 1948 in Kyoto and grew up in Osaka, Japan. He received his Ph.D. degree from the University of Tsukuba in 1979. After working as a postdoctoral fellow (1979−1981) at Brookhaven National Laboratory, he returned to the University of Tsukuba in 1981. In 1996, he moved to Niigata University as a Professor. Since 2001, he has been a Professor at the Center for Tsukuba Advanced Research Alliance (TARA Center), University of Tsukuba. His current research interests include the chemistry of fullerenes, metallofullerenes, and carbon nanotubes.

Shigeru Nagase, born in 1946 in Osaka, Japan, received his Ph.D. degree from Osaka University in 1975. After working as a postdoctoral fellow (1976−1979) at the University of Rochester and The Ohio State University, he returned to the Institute for Molecular Science in 1979. In 1980, he became an Associate Professor at Yokohama National University. He was promoted to Professor in 1991. In 1995, he moved to Tokyo Metropolitan University. Since 2001, he has been a Professor in the Department of Theoretical and Computational Molecular Science, Institute for Molecular Science. He has great interest in developing new molecules and reactions through close comparisons between theoretical predictions and results of experimental tests.

FOOTNOTES

*To whom correspondence should be addressed. E-mail: akasaka@tara.tsukuba.ac.jp (T.A.); nagase@ims.ac.jp (S.N.).

REFERENCES

1 Kroto, H. W.; Heath, J. R.; O'Brien, S. C.; Curl, R. F.; Smalley, R. E. C_{60}: Buckminsterfullerene. *Nature* **1985**, *318*, 162–163.

2 *Endofullerenes: A New Family of Carbon Clusters*; Akasaka, T., Nagase, S., Eds.; Kluwer: Dordrecht, The Netherlands, 2002.

3 Chai, Y.; Guo, T.; Jin, C.; Haufler, R. E.; Chibante, L. P. F.; Fure, J.; Wang, L.; Alford, J. M.; Smalley, R. E. Fullerenes with metals inside. *J. Phys. Chem.* **1991**, *95*, 7564–7568.

4 Kobayashi, S.; Mori, S.; Iida, S.; Ando, H.; Takenobu, T.; Taguchi, Y.; Fujiwara, A.; Taninaka, A.; Shinohara, H.; Iwasa, Y. Conductivity and field effect transistor of $La_2@C_{80}$ metallofullerene. *J. Am. Chem. Soc.* **2003**, *125*, 8116–8117.

5 Yasutake, Y.; Shi, Z.; Okazaki, T.; Shinohara, H.; Majima, Y. Single molecular orientation switching of an endohedral metallofullerene. *Nano Lett.* **2005**, *5*, 1057–1060.

6 Tsuchiya, T.; Kumashiro, R.; Tanigaki, K.; Matsunaga, Y.; Ishitsuka, M. O.; Wakahara, T.; Maeda, Y.; Takano, Y.; Aoyagi, M.; Akasaka, T.; Liu, M. T. H.; Kato, T.; Suenaga, K.; Jeong, J. S.; Iijima, S.; Kimura, F.; Kimura, T.; Nagase, S. Nanorods of endohedral metallofullerene derivative. *J. Am. Chem. Soc.* **2008**, *130*, 450–451.

7 Ross, R. B.; Cardona, C. M.; Guldi, D. M.; Sankaranarayanan, S. G.; Reese, M. O.; Kopidakis, N.; Peet, J.; Walker, B.; Bazan, G. C.; Van Keuren, E.; Holloway, B. C.; Drees, M. Endohedral fullerenes for organic photovoltaic devices. *Nat. Mater.* **2009**, *8*, 208–212.

8 Cagle, D. W.; Kennel, S. J.; Mirzadeh, S.; Alford, J. M.; Wilson, L. J. In *vivo* studies of fullerene-based materials using endohedral metallofullerene radiotracers. *Proc. Natl. Acad. Sci. U.S.A.* **1999**, *96*, 5182–5187.

9 Fatouros, P. P.; Corwin, F. D.; Chen, Z.-J.; Broaddus, W. C.; Tatum, J. L.; Kettenmann, B.; Ge, Z.; Gibson, H. W.; Russ, J. L.; Leonard, A. P.; Duchamp, J. C.; Dorn, H. C. In vitro and in vivo imaging studies of a new endohedral metallofullerene nanoparticle. *Radiology* **2006**, *240*, 756–764.

10 Akasaka, T.; Wakahara, T.; Nagase, S.; Kobayashi, K.; Waelchli, M.; Yamamoto, K.; Kondo, M.; Shirakura, S.; Okubo, S.; Maeda, Y.; Kato, T.; Kako, M.; Nakadaira, Y.; Nagahata, R.; Gao, X.; Van Caemelbecke, E.; Kadish, K. M. $La@C_{82}$ anion. An unusually stable metallofullerene. *J. Am. Chem. Soc.* **2000**, *122*, 9316–9317.

11 Akasaka, T.; Wakahara, T.; Nagase, S.; Kobayashi, K.; Waelchli, M.; Yamamoto, K.; Kondo, M.; Shirakura, S.; Maeda, Y.; Kato, T.; Kako, M.; Nakadaira, Y.; Gao, X.; Van Caemelbecke, E.; Kadish, K. M. Structural determination of the $La@C_{82}$ isomer. *J. Phys. Chem. B* **2001**, *105*, 2971–2974.

12 Wakahara, T.; Kobayashi, J.; Yamada, M.; Maeda, Y.; Tsuchiya, T.; Okamura, M.; Akasaka, T.; Waelchli, M.; Kobayashi, K.; Nagase, S.; Kato, T.; Kako, M.; Yamamoto, K.; Kadish, K. M. Characterization of $Ce@C_{82}$ and its anion. *J. Am. Chem. Soc.* **2004**, *126*, 4883–4887.

13 Wakahara, T.; Okubo, S.; Kondo, M.; Maeda, Y.; Akasaka, T.; Waelchli, M.; Kako, M.; Kobayashi, K.; Nagase, S.; Kato, T.; Yamamoto, K.; Gao, X.; Van Caemelbecke, E.; Kadish, K. M. Ionization and structural determination of the major isomer of $Pr@C_{82}$. *Chem. Phys. Lett.* **2002**, *360*, 235–239.

14 Feng, L.; Wakahara, T.; Tsuchiya, T.; Maeda, Y.; Lian, Y.; Akasaka, T.; Mizorogi, N.; Kobayashi, K.; Nagase, S.; Kadish, K. M. Structural characterization of $Y@C_{82}$. *Chem. Phys. Lett.* **2005**, *405*, 274–277.

15 Yamada, M.; Wakahara, T.; Lian, Y.; Tsuchiya, T.; Akasaka, T.; Waelchli, M.; Mizorogi, N.; Nagase, S.; Kadish, K. M. Analysis of lanthanide-induced NMR shifts of the $Ce@C_{82}$ anion. *J. Am. Chem. Soc.* **2006**, *128*, 1400–1401.

16 Bleaney, B. Nuclear magnetic resonance shifts in solution due to lanthanide ions. *J. Magn. Reson.* **1972**, *8*, 91–100.

17 Tsuchiya, T.; Wakahara, T.; Maeda, Y.; Akasaka, T.; Waelchli, M.; Kato, T.; Okubo, H.; Mizorogi, N.; Kobayashi, K.; Nagase, S. 2D NMR characterization of the $La@C_{82}$ anion. *Angew. Chem., Int. Ed.* **2005**, *44*, 3282–3285.

18 Kobayashi, K.; Nagase, S. Structures and electronic states of $M@C_{82}$ (M = Sc, Y, La and lanthanides). *Chem. Phys. Lett.* **1998**, *282*, 325–329.

19 Akasaka, T.; Kato, T.; Kobayashi, K.; Nagase, S.; Yamamoto, K.; Funasaka, H.; Takahashi, T. Exohedral adducts of $La@C_{82}$. *Nature* **1995**, *374*, 600.

20 Yamada, M.; Feng, L.; Wakahara, T.; Tsuchiya, T.; Maeda, Y.; Lian, Y.; Kako, M.; Akasaka, T.; Kato, T.; Kobayashi, K.; Nagase, S. Synthesis and characterization of exohedrally silylated $M@C_{82}$ (M = Y and La). *J. Phys. Chem. B* **2005**, *109*, 6049–6051.

21 Maeda, Y.; Matsunaga, Y.; Wakahara, T.; Takahashi, S.; Tsuchiya, T.; Ishitsuka, M. O.; Hasegawa, T.; Akasaka, T.; Liu, M. T. H.; Kokura, K.; Horn, E.; Yoza, K.; Kato, T.; Okubo, S.; Kobayashi, K.; Nagase, S.; Yamamoto, K. Isolation and characterization of a carbene derivative of $La@C_{82}$. *J. Am. Chem. Soc.* **2004**, *126*, 6858–6859.

22 Akasaka, T.; Kono, T.; Takematsu, Y.; Nikawa, H.; Nakahodo, T.; Wakahara, T.; Ishitsuka, M. O.; Tsuchiya, T.; Maeda, Y.; Liu, M. T. H.; Yoza, K.; Kato, T.; Yamamoto, K.; Mizorogi, N.; Slanina, Z.; Nagase, S. Does $Gd@C_{82}$ have an anomalous endohedral structure? Synthesis and single crystal x-ray structure of the carbene adduct. *J. Am. Chem. Soc.* **2008**, *130*, 12840–12841.

23 Senapati, L.; Schrier, J.; Whaley, K. B. Electronic transport, structure, and energetics of endohedral $Gd@C_{82}$ metallofullerenes. *Nano Lett.* **2004**, *4*, 2073–2078.

24 Senapati, L.; Schrier, J.; Whaley, K. B. Reply to comment on "electronic transport, structure, and energetics of endohedral $Gd@C_{82}$ metallofullerenes". *Nano Lett.* **2005**, *5*, 2341–2341.

25 Mizorogi, N.; Nagase, S. Do $Eu@C_{82}$ and $Gd@C_{82}$ have an anomalous endohedral structure? *Chem. Phys. Lett.* **2006**, *431*, 110–112.

26 Liu, L.; Gao, B.; Chu, W.; Chen, D.; Hu, T.; Wang, C.; Dunsch, L.; Marcelli, A.; Luo, Y.; Wu, Z. The structural determination of endohedral metallofullerene $Gd@C_{82}$ by XANES. *Chem. Commun.* **2008**, 474–476.

27 Nishibori, E.; Iwata, K.; Sakata, M.; Takata, M.; Tanaka, H.; Kato, H.; Shinohara, H. Anomalous endohedral structure of $Gd@C_{82}$ metallofullerenes. *Phys. Rev. B: Condens. Matter Mater. Phys.* **2004**, *69*, 113412(1−4) .

28 Feng, L.; Nakahodo, T.; Wakahara, T.; Tsuchiya, T.; Maeda, Y.; Akasaka, T.; Kato, T.; Horn, E.; Yoza, K.; Mizorogi, N.; Nagase, S. A singly bonded derivative of endohedral metallofullerene: $La@C_{82}CBr(COOC_2H_5)_2$. *J. Am. Chem. Soc.* **2005**, *127*, 17136–17137.

29 Feng, L.; Wakahara, T.; Nakahodo, T.; Tsuchiya, T.; Piao, Q.; Maeda, Y.; Lian, Y.; Akasaka, T.; Horn, E.; Yoza, K.; Kato, T.; Mizorogi, N.; Nagase, S. The bingel monoadducts of $La@C_{82}$: Synthesis, characterization, and electrochemistry. *Chem.—Eur. J.* **2006**, *12*, 5578–5586.

30 Feng, L.; Tsuchiya, T.; Wakahara, T.; Nakahodo, T.; Piao, Q.; Maeda, Y.; Akasaka, T.; Kato, T.; Yoza, K.; Horn, E.; Mizorogi, N.; Nagase, S. Synthesis and characterization of a bisadduct of $La@C_{82}$. *J. Am. Chem. Soc.* **2006**, *128*, 5990–5991.

31 Takano, Y.; Yomogida, A.; Nikawa, H.; Yamada, M.; Wakahara, T.; Tsuchiya, T.; Ishitsuka, M. O.; Maeda, Y.; Akasaka, T.; Kato, T.; Slanina, Z.; Mizorogi, N.; Nagase, S. Radical coupling reaction of paramagnetic endohedral metallofullerene $La@C_{82}$. *J. Am. Chem. Soc.* **2008**, *130*, 16224–16230.

32 Dunsch, L.; Bartl, A.; Georgi, P.; Kuran, P. New metallofullerenes in the size gap of C_{70} to C_{82}: From $La_2@C_{72}$ to $Sc_3N@C_{80}$. *Synth. Met.* **2001**, *121*, 1113–1114.

33 Yamada, M.; Wakahara, T.; Tsuchiya, T.; Maeda, Y.; Akasaka, T.; Mizorogi, N.; Nagase, S. Spectroscopic and theoretical study of endohedral dimetallofullerene having a non-IPR fullerene cage: $Ce_2@C_{72}$. *J. Phys. Chem. A* **2008**, *112*, 7627–7631.

34 Yamada, M.; Wakahara, T.; Tsuchiya, T.; Maeda, Y.; Kako, M.; Akasaka, T.; Yoza, K.; Horn, E.; Mizorogi, N.; Nagase, S. Location of the metal atoms in $Ce_2@C_{78}$ and its bis-silylated derivative. *Chem. Commun.* **2008**, 558–560.

35 Akasaka, T.; Nagase, S.; Kobayashi, K.; Waelchli, M.; Yamamoto, K.; Funasaka, H.; Kako, M.; Hoshino, T.; Erata, T. ^{13}C and ^{139}La NMR studies of $La_2@C_{80}$: First evidence for circular motion of metal atoms in endohedral metallofullerenes. *Angew. Chem., Int. Ed. Engl.* **1997**, *36*, 1643–1645.

36 Wakahara, T.; Yamada, M.; Takahashi, S.; Nakahodo, T.; Tsuchiya, T.; Maeda, Y.; Akasaka, T.; Kako, M.; Yoza, K.; Horn, E.; Mizorogi, N.; Nagase, S. Two-dimensional hopping motion of encapsulated La atoms in silylated $La_2@C_{80}$. *Chem. Commun.* **2007**, 2680–2682.

37 Kobayashi, K.; Nagase, S.; Akasaka, T. Endohedral dimetallofullerenes $Sc_2@C_{84}$ and $La_2@C_{80}$. Are the metal atoms still inside the fullerene cages? *Chem. Phys. Lett.* **1996**, *261*, 502–506.

38 Shimotani, H.; Ito, T.; Iwasa, Y.; Taninaka, A.; Shinohara, H.; Nishibori, E.; Takata, M.; Sakata, M. Quantum chemical study on the configurations of encapsulated metal ions and the molecular vibration modes in endohedral dimetallofullerene $La_2@C_{80}$. *J. Am. Chem. Soc.* **2004**, *126*, 364–369.

39 Zhang, J.; Hao, C.; Li, S.; Mi, W.; Jin, P. Which configuration is more stable for $La_2@C_{80}$, D_{3d} or D_{2h}? Recomputation with ZORA methods within ADF. *J. Phys. Chem. C* **2007**, *111*, 7862–7867.

40 Yamada, M.; Nakahodo, T.; Wakahara, T.; Tsuchiya, T.; Maeda, Y.; Akasaka, T.; Kako, M.; Yoza, K.; Horn, E.; Mizorogi, N.; Kobayashi, K.; Nagase, S. Positional control of encapsulated atoms inside a fullerene cage by exohedral addition. *J. Am. Chem. Soc.* **2005**, *127*, 14570–14571.

41 Yamada, M.; Mizorogi, N.; Tsuchiya, T.; Akasaka, T.; Nagase, S. Synthesis and characterization of the D_{5h} isomer of the endohedral dimetallofullerene $Ce_2@C_{80}$: Two-dimensional circulation of encapsulated metal atoms inside a fullerene cage. *Chem.—Eur. J.* **2009**, in press.

42 Lu, X.; Nikawa, H.; Nakahodo, T.; Tsuchiya, T.; Ishitsuka, M. O.; Maeda, Y.; Akasaka, T.; Toki, M.; Sawa, H.; Slanina, Z.; Mizorogi, N.; Nagase, S. Chemical understanding of a non-IPR metallofullerene: Stabilization of encaged metals on fused-pentagon bonds in $La_2@C_{72}$. *J. Am. Chem. Soc.* **2008**, *130*, 9129–9136.

43 Lu, X.; Nikawa, H.; Tsuchiya, T.; Maeda, Y.; Ishitsuka, M. O.; Akasaka, T.; Toki, M.; Sawa, H.; Slanina, Z.; Mizorogi, N.; Nagase, S. Bis-carbene adducts of non-IPR $La_2@C_{72}$: Localization of high reactivity around fused pentagons and electrochemical properties. *Angew. Chem., Int. Ed.* **2008**, *47*, 8642–8645.

44 Cao, B.; Nikawa, H.; Nakahodo, T.; Tsuchiya, T.; Maeda, Y.; Akasaka, T.; Sawa, H.; Slanina, Z.; Mizorogi, N.; Nagase, S. Addition of adamantylidene to $La_2@C_{78}$: Isolation and single-crystal x-ray structural determination of the monoadducts. *J. Am. Chem. Soc.* **2008**, *130*, 983–989.

45 Cao, B.; Wakahara, T.; Tsuchiya, T.; Kondo, M.; Maeda, Y.; Rahman, G. M. A.; Akasaka, T.; Kobayashi, K.; Nagase, S.; Yamamoto, K. Isolation, characterization, and theoretical study of $La_2@C_{78}$. *J. Am. Chem. Soc.* **2004**, *126*, 9164–9165.

46 Kobayashi, K.; Nagase, S.; Maeda, Y.; Wakahara, T.; Akasaka, T. $La_2@C_{80}$: Is the circular motion of two La atoms controllable by exohedral addition? *Chem. Phys. Lett.* **2003**, *374*, 562–566.

47 Yamada, M.; Wakahara, T.; Nakahodo, T.; Tsuchiya, T.; Maeda, Y.; Akasaka, T.; Yoza, K.; Horn, E.; Mizorogi, N.; Nagase, S. Synthesis and structural characterization of endohedral pyrrolidinodimetallofullerene: $La_2@C_{80}(CH_2)_2NTrt$. *J. Am. Chem. Soc.* **2006**, *128*, 1402–1403.

48 Yamada, M.; Okamura, M.; Sato, S.; Someya, C. I.; Mizorogi, N.; Tsuchiya, T.; Akasaka, T.; Kato, T.; Nagase, S. Two regioisomers of endohedral pyrrolidinodimetallofullerenes $M_2@I_h-C_{80}(CH_2)_2NTrt$ (M = La, Ce; Trt = trityl): Control of metal atom positions by addition positions. *Chem.—Eur. J.* **2009**, manuscript accepted.

49 Yamada, M.; Someya, C.; Wakahara, T.; Tsuchiya, T.; Maeda, Y.; Akasaka, T.; Yoza, K.; Horn, E.; Liu, M. T. H.; Mizorogi, N.; Nagase, S. Metal atoms collinear with the spiro carbon of 6,6-open adducts, $M_2@C_{80}$(Ad) (M = La and Ce, Ad = adamantylidene). *J. Am. Chem. Soc.* **2008**, *130*, 1171–1176.

50 Iiduka, Y.; Ikenaga, O.; Sakuraba, A.; Wakahara, T.; Tsuchiya, T.; Maeda, Y.; Nakahodo, T.; Akasaka, T.; Kako, M.; Mizorogi, N.; Nagase, S. Chemical reactivity of $Sc_3N@C_{80}$ and $La_2@C_{80}$. *J. Am. Chem. Soc.* **2005**, *127*, 9956–9957.

51 Wakahara, T.; Iiduka, Y.; Ikenaga, O.; Nakahodo, T.; Sakuraba, A.; Tsuchiya, T.; Maeda, Y.; Kako, M.; Akasaka, T.; Yoza, K.; Horn, E.; Mizorogi, N.; Nagase, S. Characterization of the bis-silylated endofullerene $Sc_3N@C_{80}$. *J. Am. Chem. Soc.* **2006**, *128*, 9919–9925.

52 Iiduka, Y.; Wakahara, T.; Nakahodo, T.; Tsuchiya, T.; Sakuraba, A.; Maeda, Y.; Akasaka, T.; Yoza, K.; Horn, E.; Kato, T.; Liu, M. T. H.; Mizorogi, N.; Kobayashi, K.; Nagase, S. Structural determination of metallofullerene Sc_3C_{82} revisited: A surprising finding. *J. Am. Chem. Soc.* **2005**, *127*, 12500–12501.

53 Iiduka, Y.; Wakahara, T.; Nakajima, K.; Nakahodo, T.; Tsuchiya, T.; Maeda, Y.; Akasaka, T.; Yoza, K.; Liu, M. T. H.; Mizorogi, N.; Nagase, S. Experimental and theoretical studies of the scandium carbide endohedral metallofullerene $Sc_2C_2@C_{82}$ and its carbene derivative. *Angew. Chem., Int. Ed.* **2007**, *46*, 5562–5564.

54 Cai, T.; Slebodnick, C.; Xu, L.; Harich, K.; Glass, T. E.; Chancellor, C.; Fettinger, J. C.; Olmstead, M. M.; Balch, A. L.; Gibson, H. W.; Dorn, H. C. A pirouette on a metallofullerene sphere: Interconversion of isomers of *N*-tritylpyrrolidino I_h $Sc_3N@C_{80}$. *J. Am. Chem. Soc.* **2006**, *128*, 6486–6492.